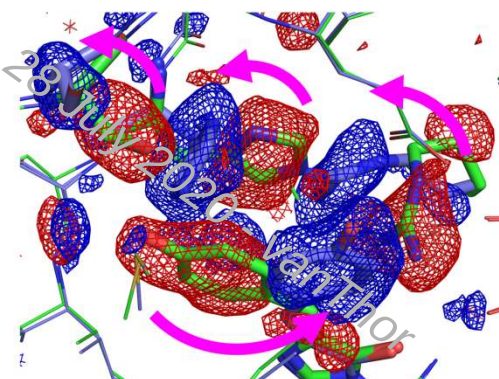
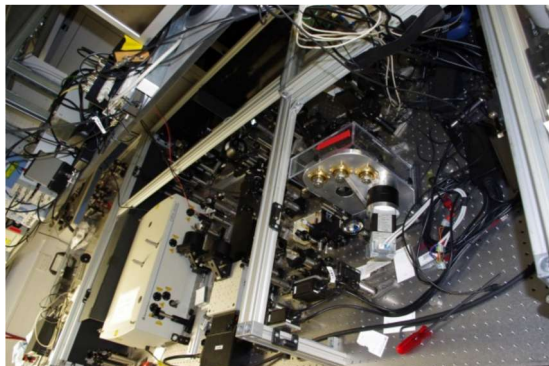
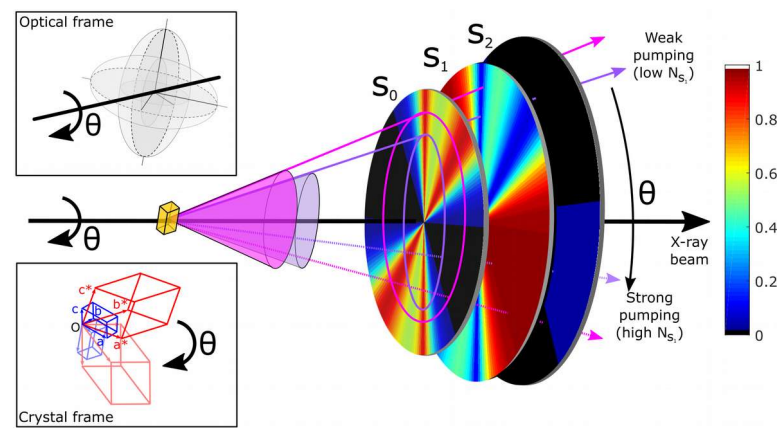
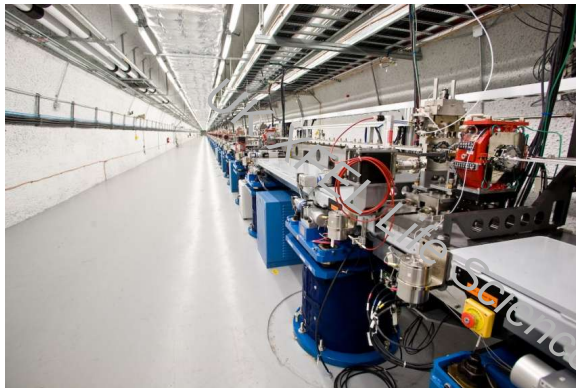
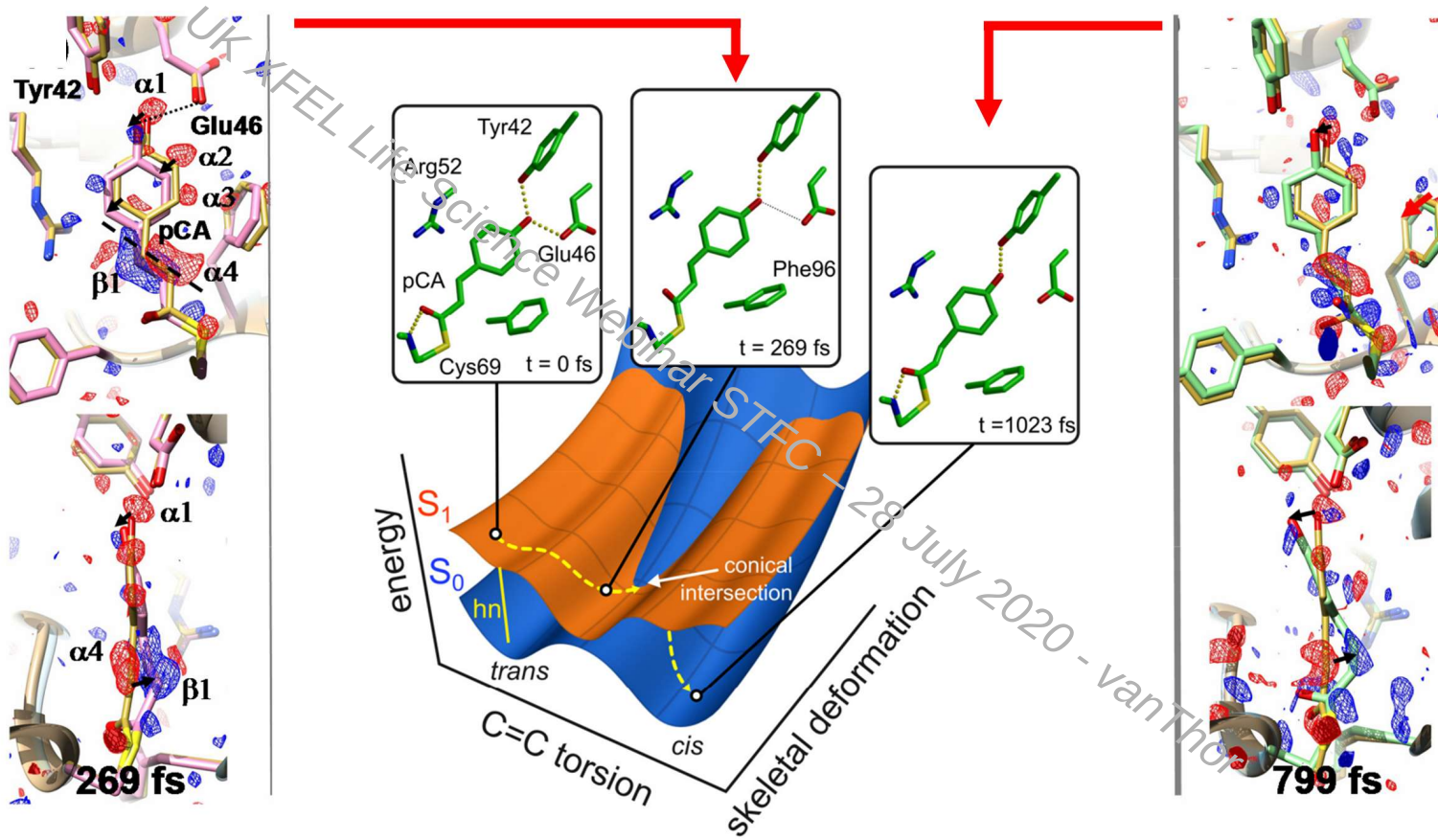


Opportunities in femtosecond time resolved protein crystallography



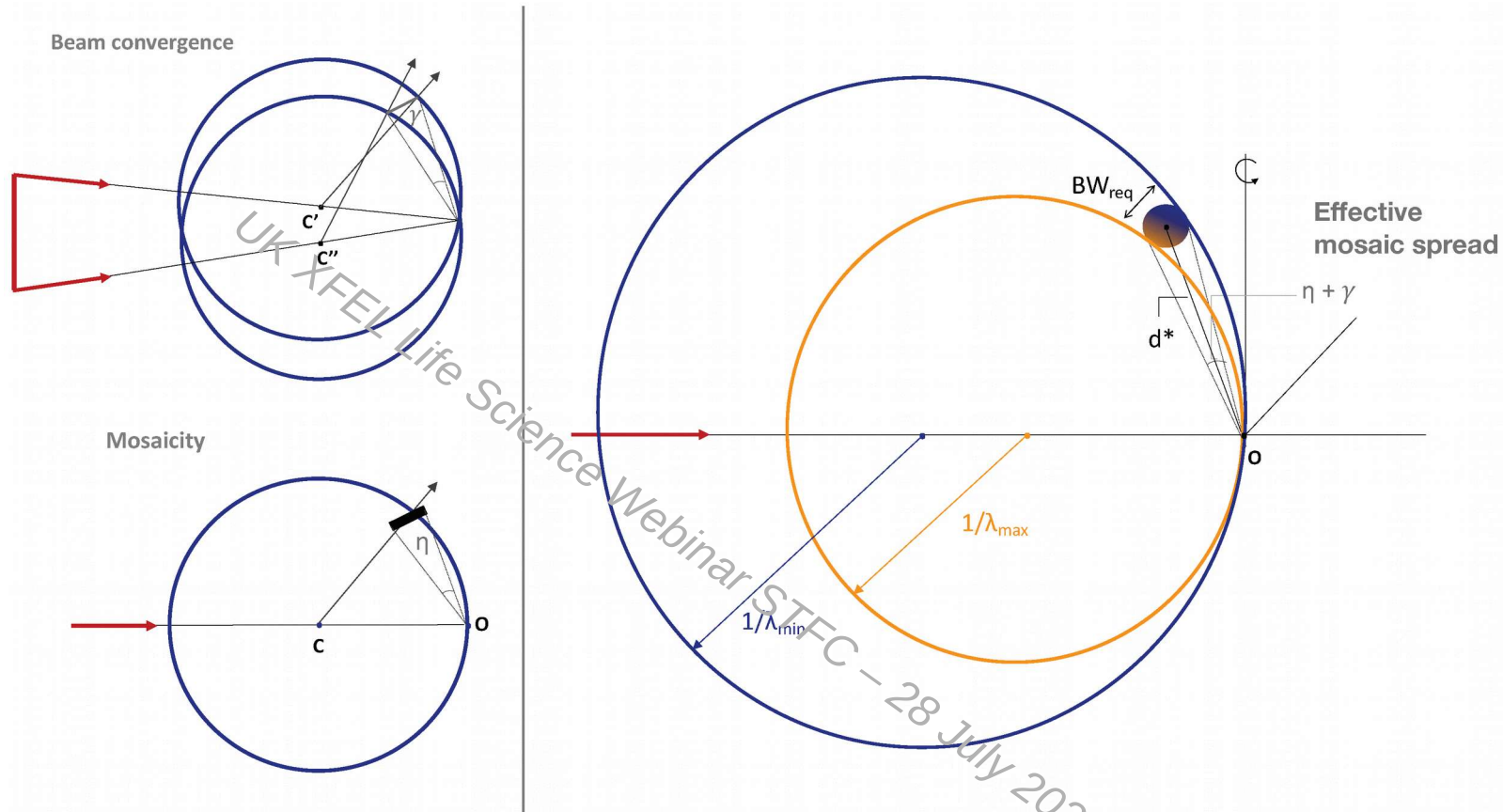
A structural view of ultrafast reaction dynamics



Control of FEL radiation

UK XFEL Life Science Webinar STFC – 28 July 2020 - vanThor

Possibility for energy-chirped ultrafast time resolved diffraction: Exploiting time-to-energy mapping of shaped XFEL pulses



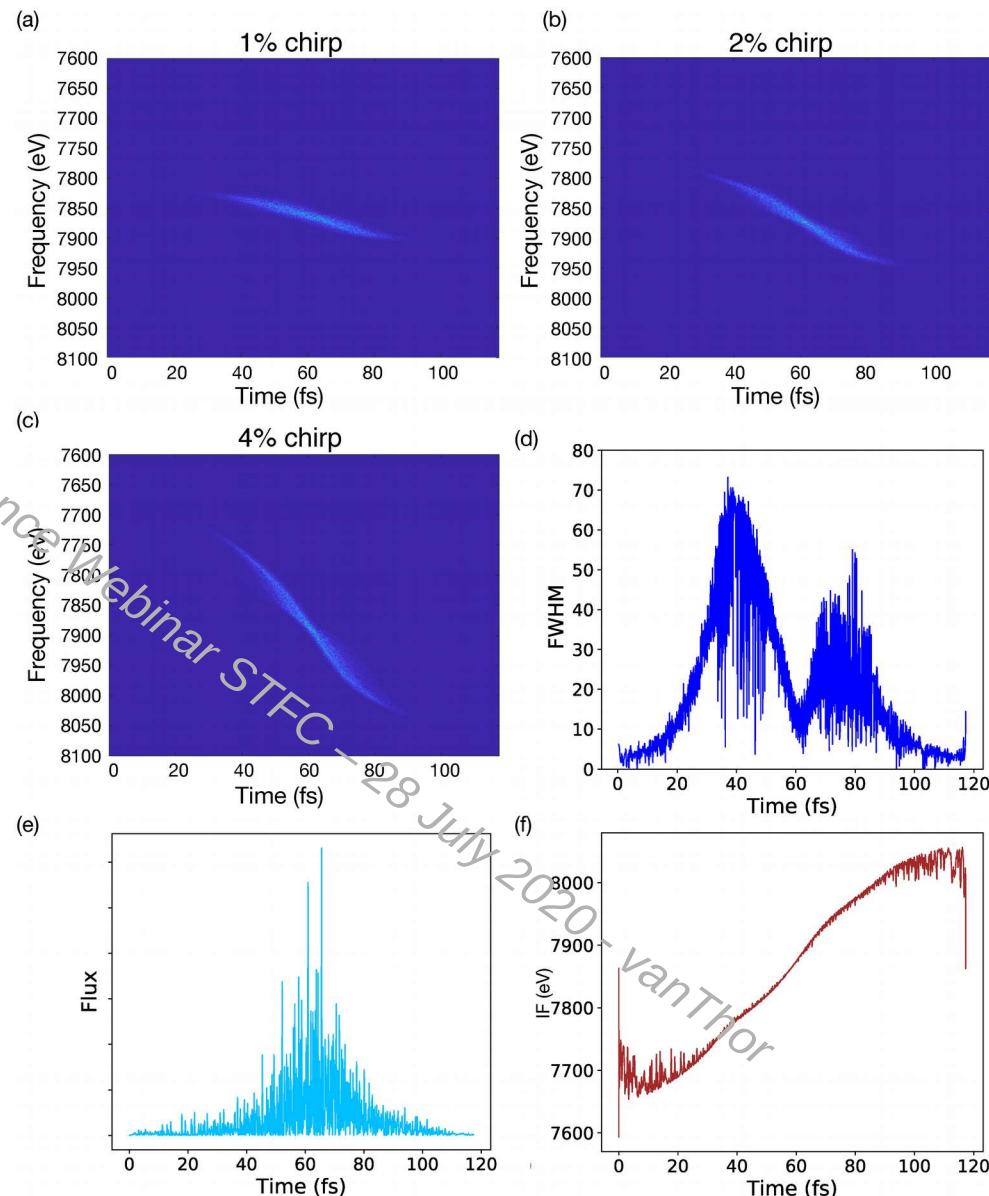
Fadini et al. Appl. Sci. 2020, 10, 2599

Effect of beam convergence (γ) and mosaicity (η) on the reflection bandwidth (BW_{req}). BW_{req} depends on the sum of γ and η and on the distance of the reciprocal lattice point from the reciprocal space origin (d^*). The minimum (λ_{min}) and maximum (λ_{max}) wavelengths of the spot bandwidth are shown together with the energy gradient across the reflection.

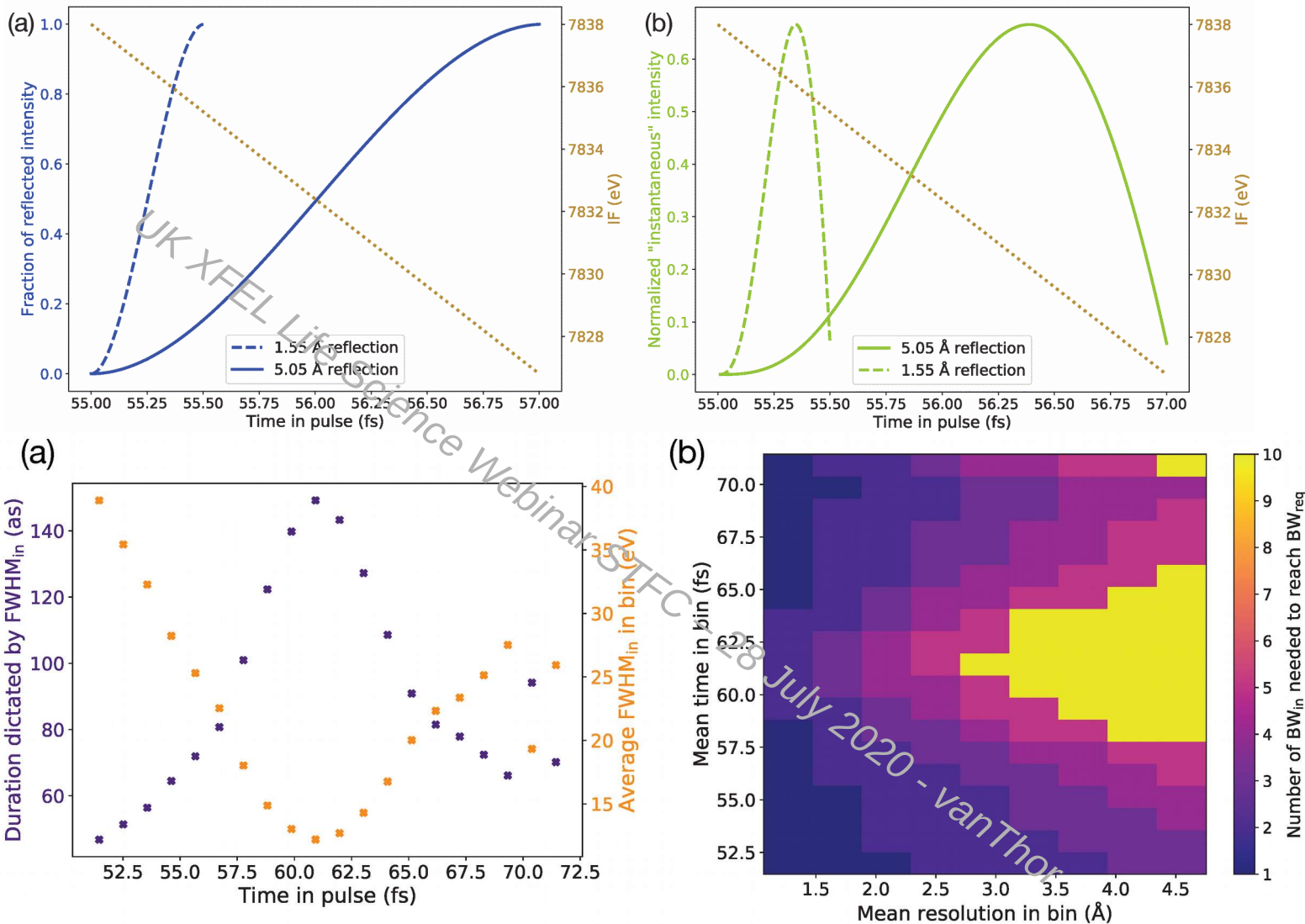
Possibility for *energy-chirped* ultrafast time resolved diffraction: Exploiting time-to-energy mapping of shaped XFEL pulses

Simulations for SwissFEL
chirped polychromatic mode

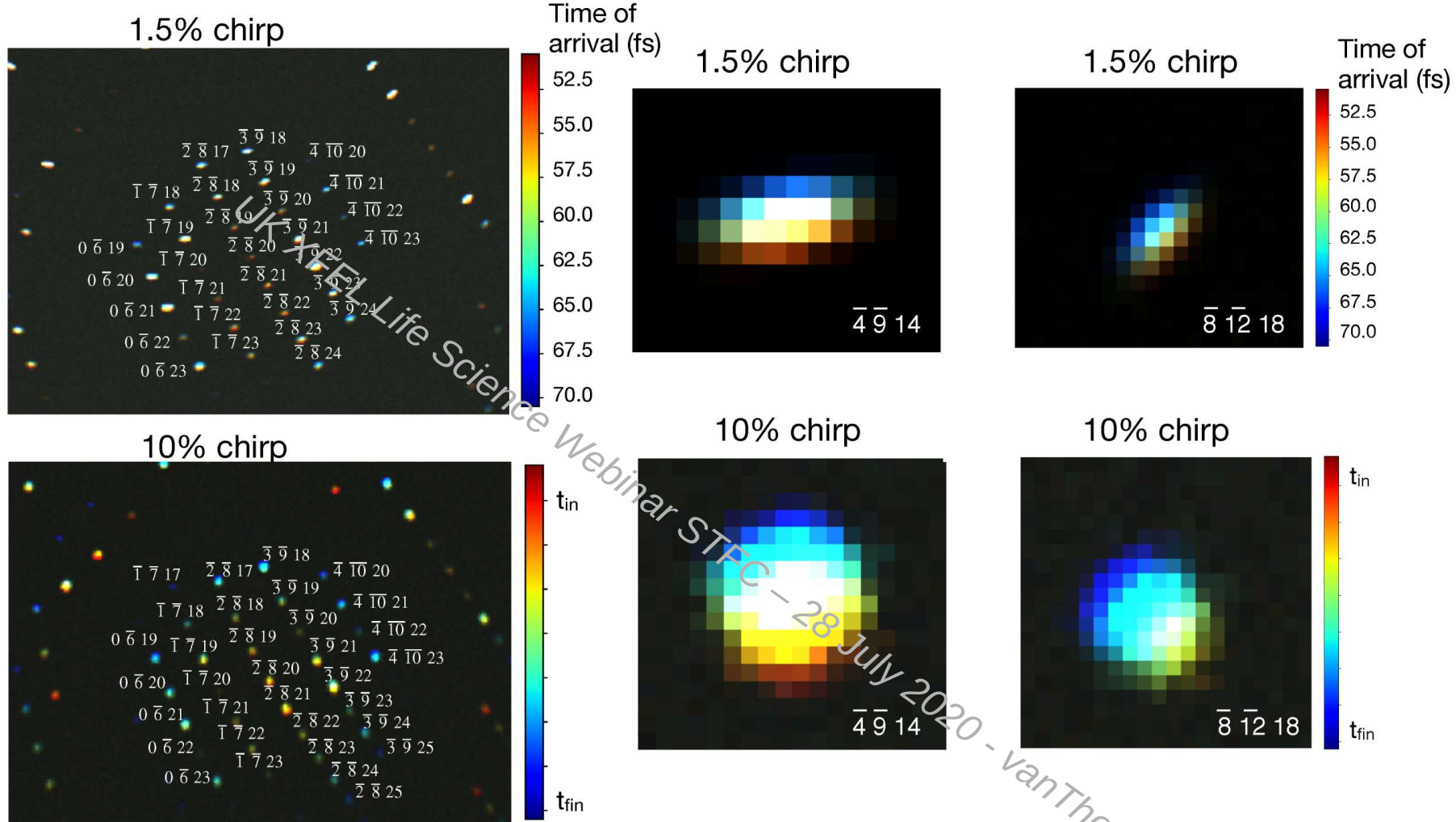
Also now experimentally
shown



Possibility for energy-chirped ultrafast time resolved diffraction: Exploiting time-to-energy mapping of shaped XFEL pulses



Possibility for *energy-chirped* ultrafast time resolved diffraction: Exploiting time-to-energy mapping of shaped XFEL pulses

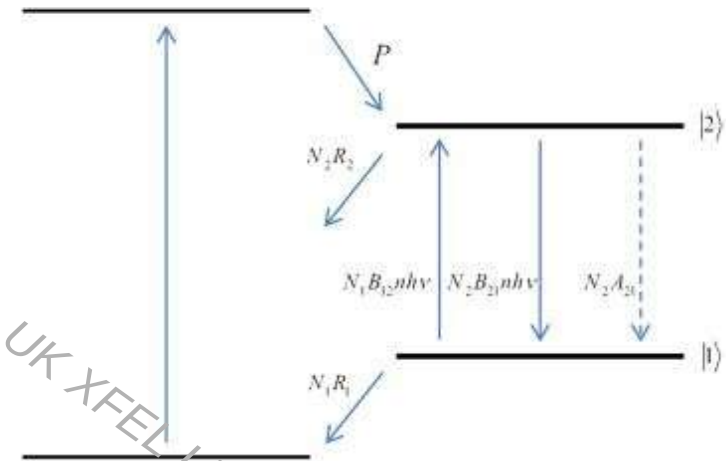


Ultrafast population dynamics analysis:

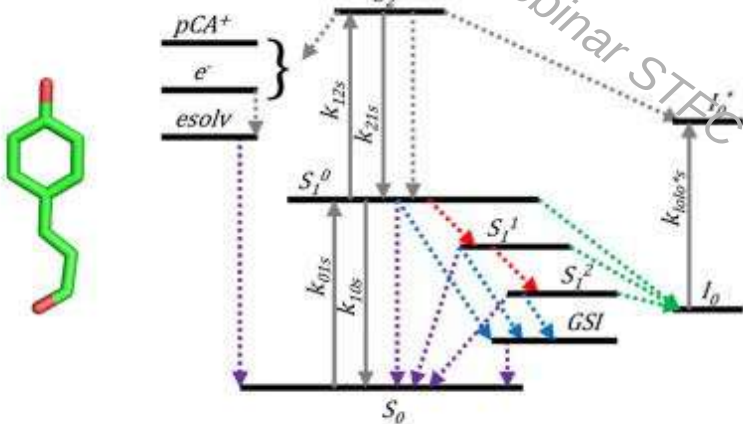
Exploiting signal-to-noise development

UK XFEL Life Science Webinar STFC – 28 July 2020 - van Thor

A) Laser rate equations for a 4-level system



B) Rate equations for a photochemical model for PYP



$$\begin{aligned}\frac{dN_1}{dt} &= (N_2 - N_1)B_{21}n\hbar\nu + N_2A_{21} - N_1R_1 \\ \frac{dN_2}{dt} &= P - (N_2 - N_1)B_{21}n\hbar\nu - N_2A_{21} - N_2R \\ \frac{dn}{dt} &= -\beta n + (N_2 - N_1)B_{21}n\hbar\nu\end{aligned}$$

$$\begin{aligned}\frac{d[S_1^0]}{dt} &= k_{01s}(t)[S_0] - k_{10s}(t)[S_1^0] - k_{12s}(t)[S_1^0] \\ &\quad + k_{21s}(t)[S_2] - \varphi_{S_1^0 \rightarrow S_1^0} k_{s_1^0}[S_1^0] \\ &\quad - \varphi_{S_1^0 \rightarrow I_0} k_{s_1^0}[S_1^0] - \varphi_{S_1^0 \rightarrow S_{GSI}} k_{s_1^0}[S_1^0] \\ &\quad - \varphi_{S_1^0 \rightarrow S_0} k_{s_1^0}[S_1^0]\end{aligned}$$

$$\begin{aligned}\frac{d[S_1^1]}{dt} &= \varphi_{S_1^0 \rightarrow S_1^1} k_{s_1^0}[S_1^0] - \varphi_{S_1^1 \rightarrow S_1^1} k_{s_1^1}[S_1^1] - \varphi_{S_1^1 \rightarrow I_0} k_{s_1^1}[S_1^1] \\ &\quad - \varphi_{S_1^1 \rightarrow S_{GSI}} k_{s_1^1}[S_1^1] - \varphi_{S_1^1 \rightarrow S_0} k_{s_1^1}[S_1^1]\end{aligned}$$

$$\begin{aligned}\frac{d[S_1^2]}{dt} &= \varphi_{S_1^1 \rightarrow S_1^2} k_{s_1^1}[S_1^1] - \varphi_{S_1^2 \rightarrow I_0} k_{s_1^2}[S_1^2] \\ &\quad - \varphi_{S_1^2 \rightarrow S_{GSI}} k_{s_1^2}[S_1^2] - \varphi_{S_1^2 \rightarrow S_0} k_{s_1^2}[S_1^2]\end{aligned}$$

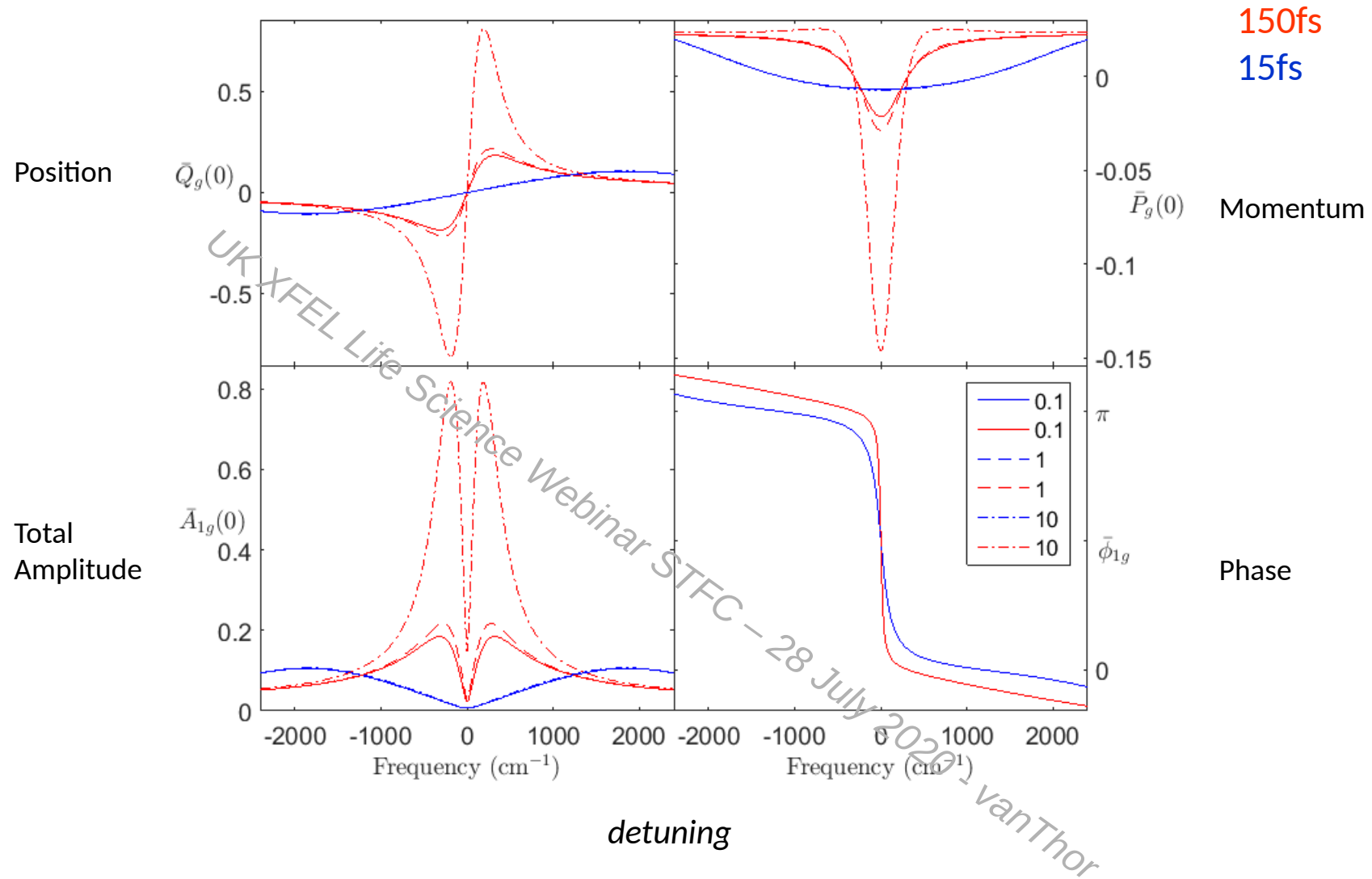
$$\begin{aligned}\frac{d[I_0]}{dt} &= \varphi_{S_1^0 \rightarrow I_0} k_{s_1^0}[S_1^0] + \varphi_{S_1^1 \rightarrow I_0} k_{s_1^1}[S_1^1] + \varphi_{S_1^2 \rightarrow I_0} k_{s_1^2}[S_1^2] \\ &\quad - k_{I_0}[I_0]\end{aligned}$$

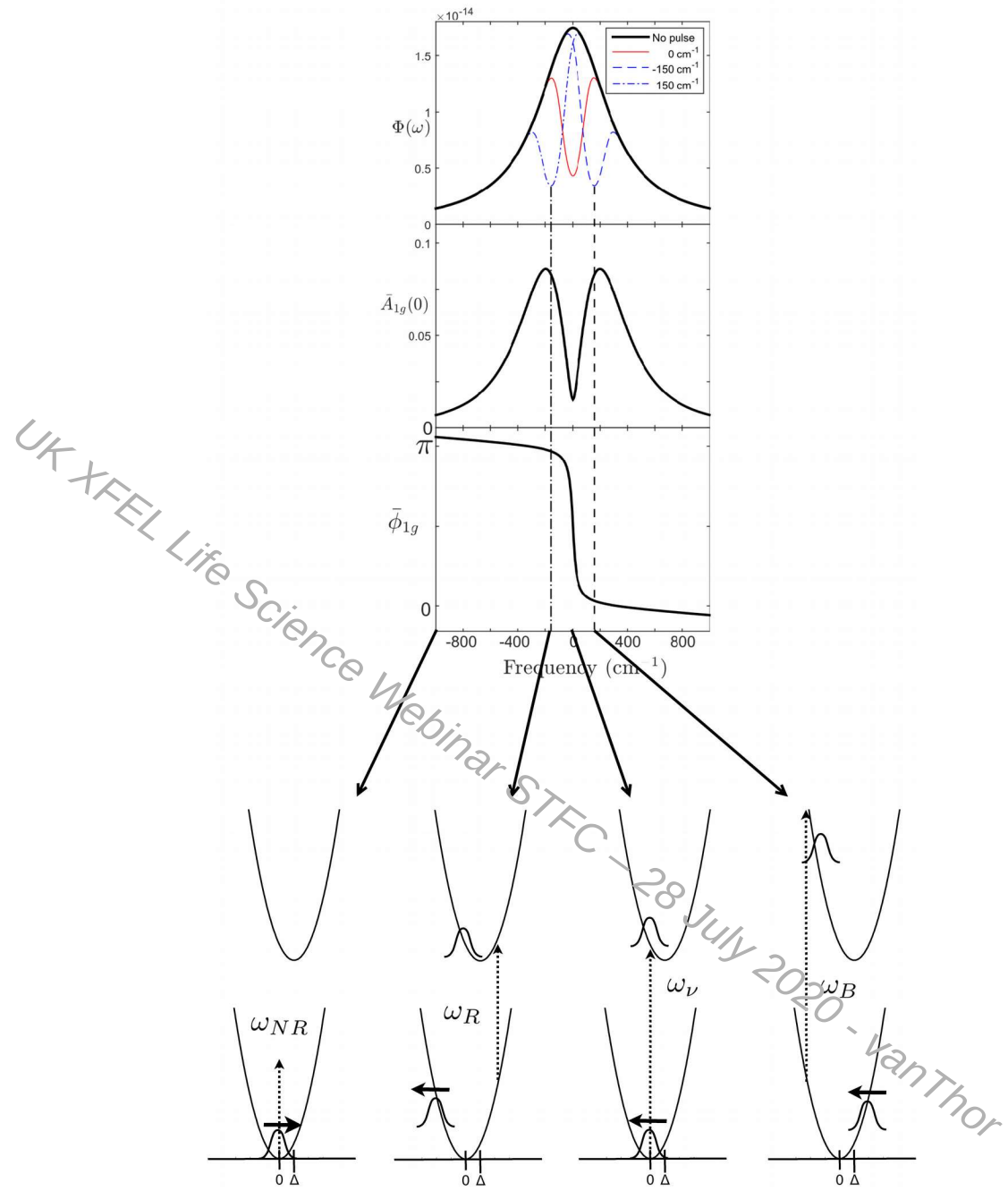
$$\begin{aligned}\frac{d[S_{GSI}]}{dt} &= \varphi_{S_1^0 \rightarrow S_{GSI}} k_{s_1^0}[S_1^0] + \varphi_{S_1^1 \rightarrow S_{GSI}} k_{s_1^1}[S_1^1] \\ &\quad + \varphi_{S_1^2 \rightarrow S_{GSI}} k_{s_1^2}[S_1^2] - k_{S_{GSI}}[S_{GSI}]\end{aligned}$$

$$\begin{aligned}\frac{d[S_2]}{dt} &= k_{12s}(t)[S_1^0] - k_{21s}(t)[S_2] - \varphi_{S_2 \rightarrow e^-} k_{s_2}[S_2] \\ &\quad - \varphi_{S_2 \rightarrow S_0} k_{s_2}[S_2]\end{aligned}$$

$$\frac{d[e^-]}{dt} = \varphi_{S_2 \rightarrow e^-} k_{s_2}[S_2]$$

Linear response theory estimates the magnitude of ground state coherence





The consequences of crystal optics

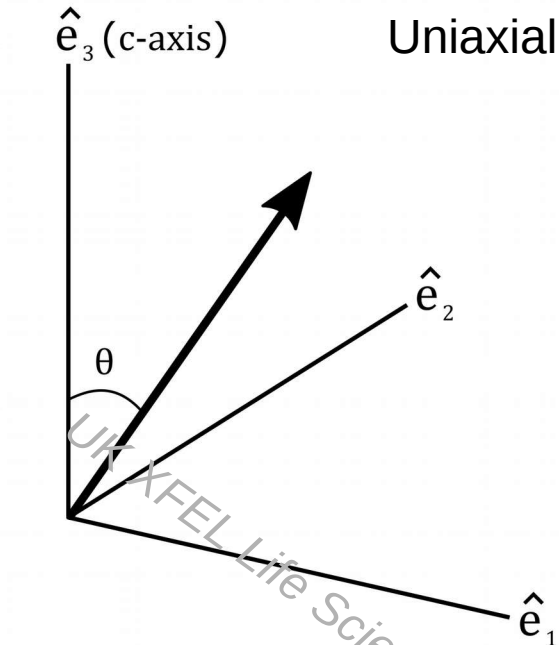
-

populations and coherence

UK XFEL Life science Webinar STFC - 28 July 2020 - van Thor

\hat{e}_3 (c-axis)

Uniaxial

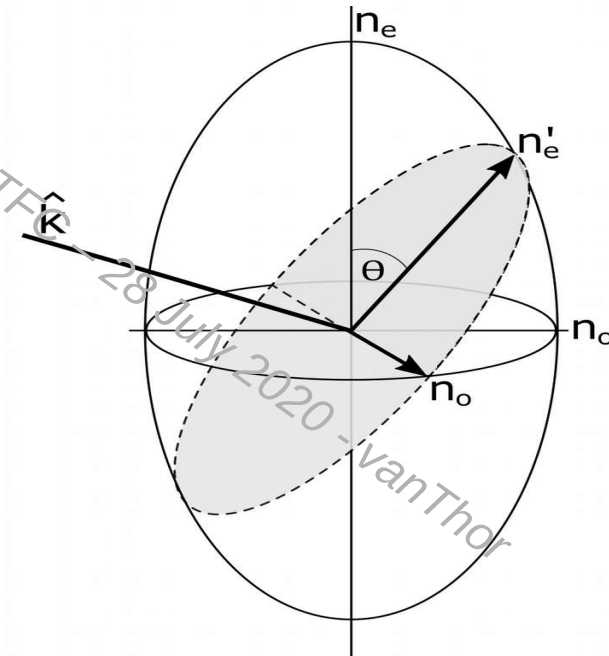
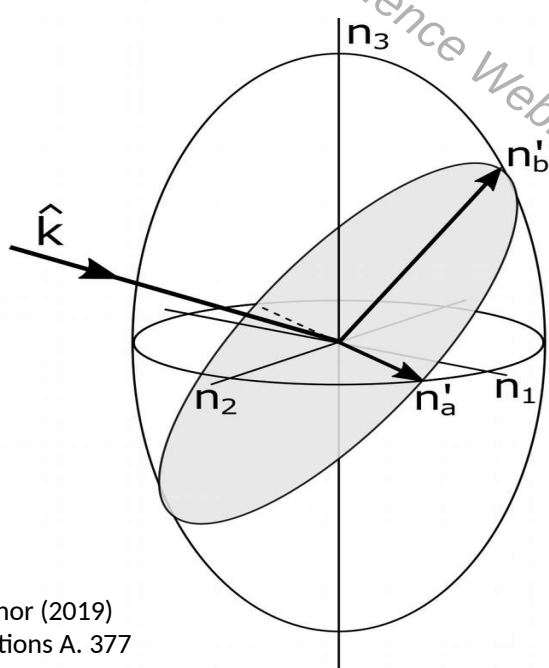
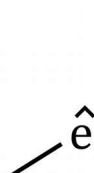


Biaxial

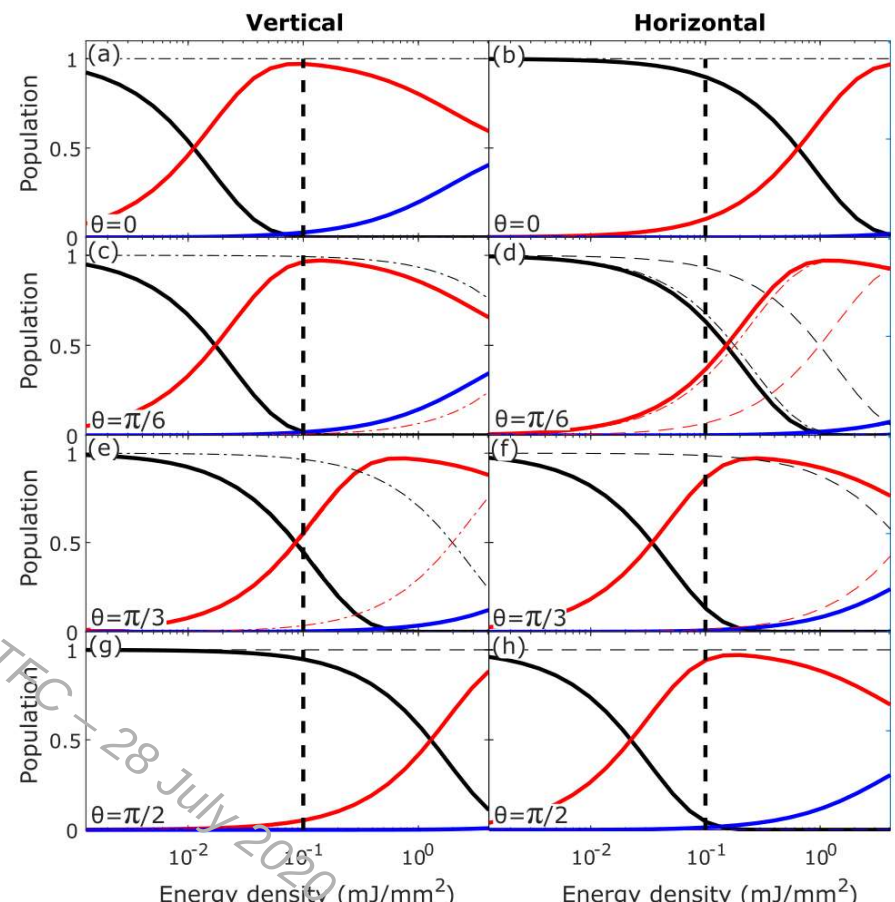
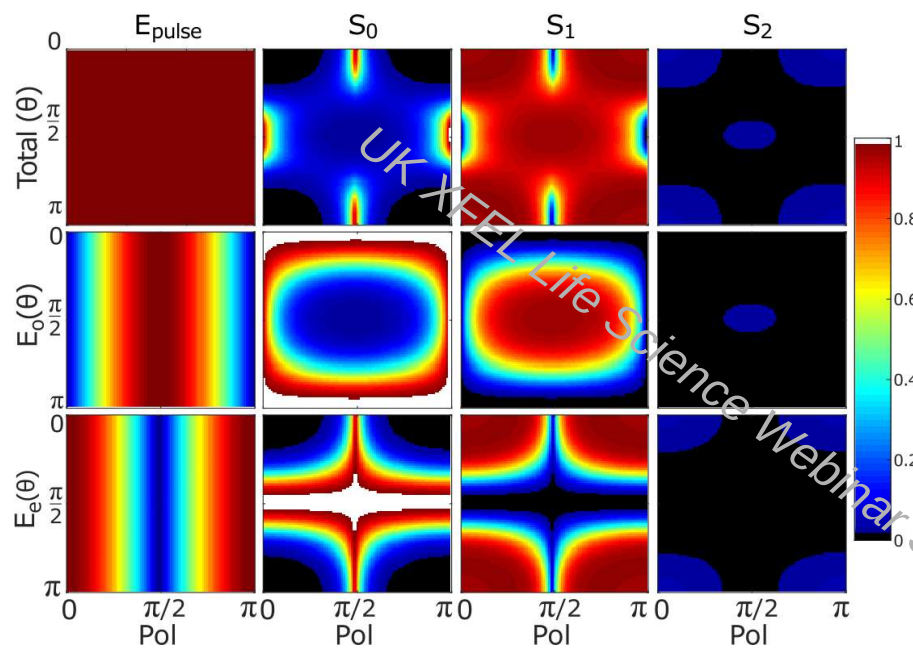
\hat{e}_3

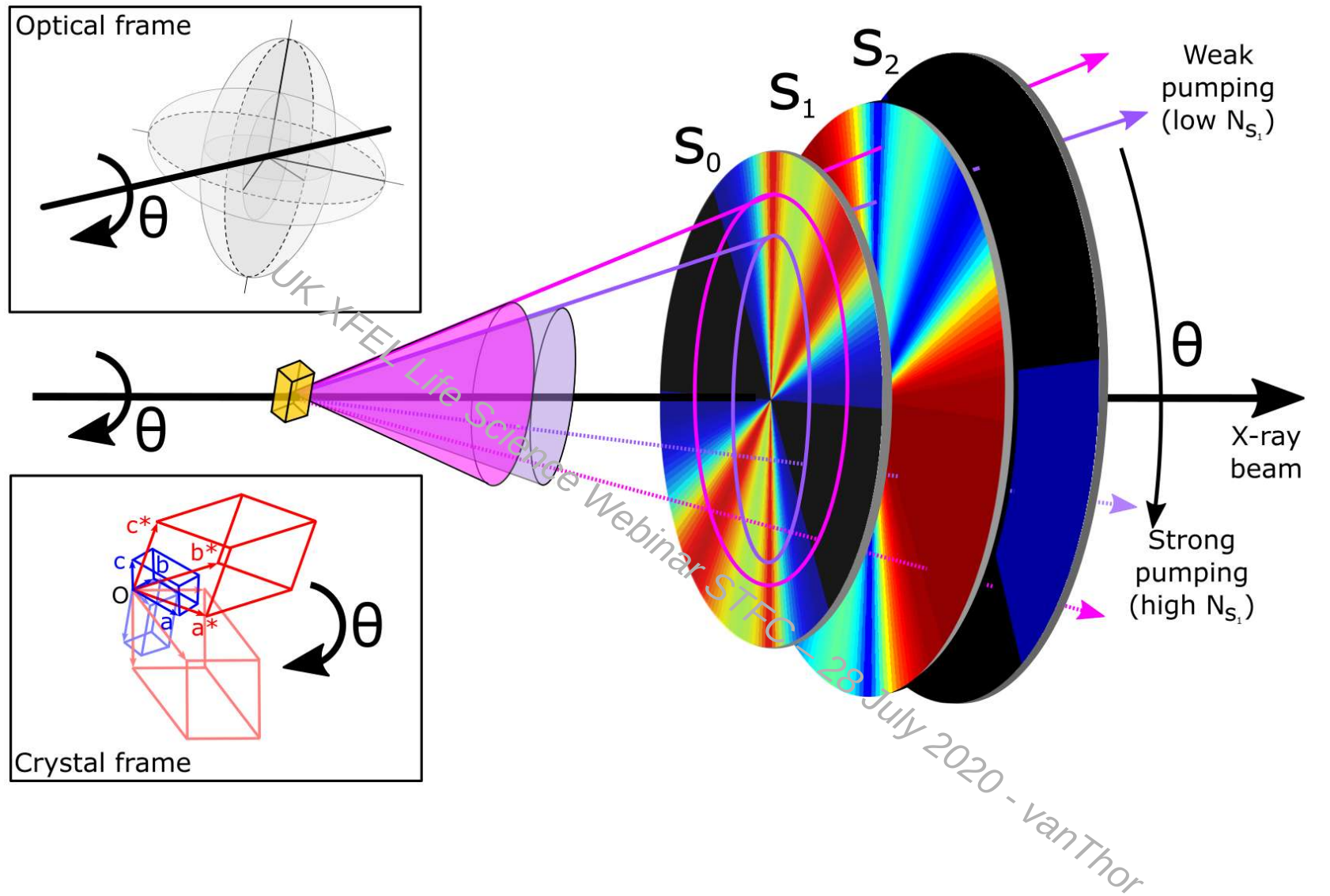
$\delta_{\alpha j}$

$\psi_{\alpha j}$

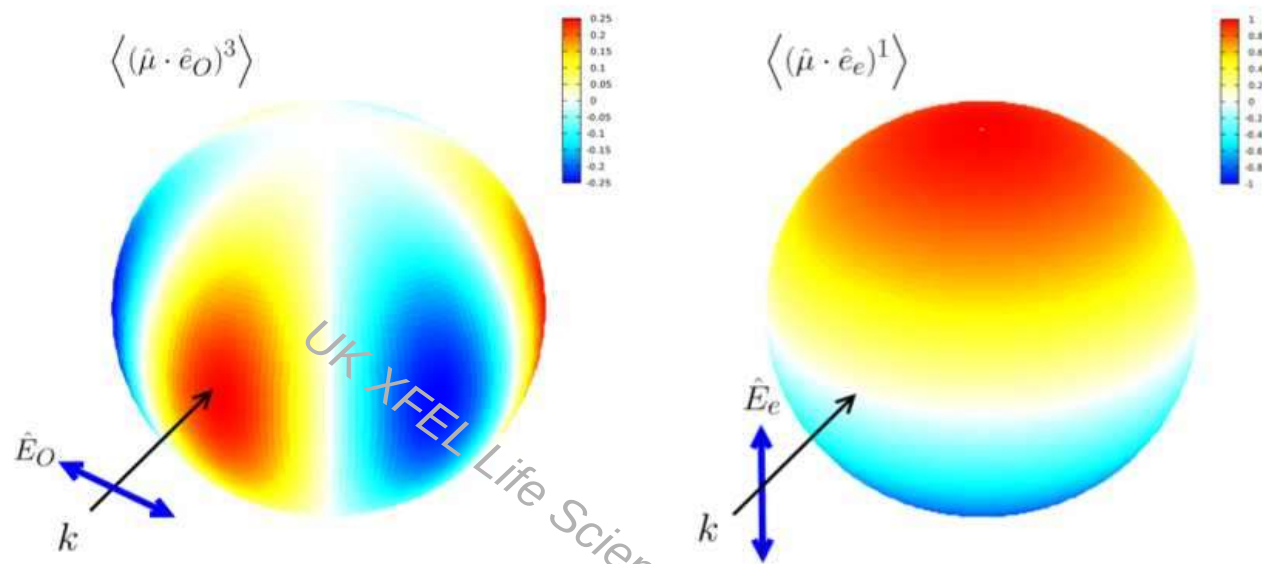


For each orientation a linear combination of two fields prepares the populations



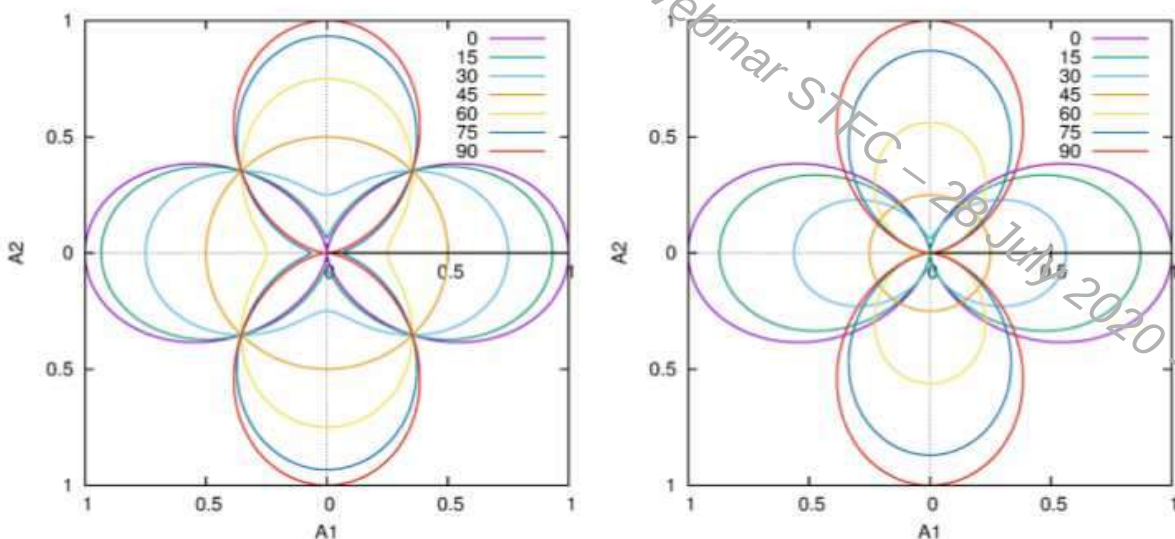


The real-space relationship to the third order response



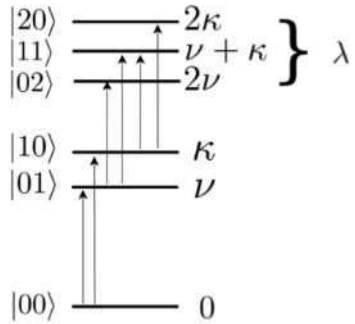
Uniaxial example

FIG. 5. A real-space plot of the third order response of an isolated oscillator with combination of three interactions in the ordinary directions (left) and a single interaction in the extraordinary direction (right) in the presence of trigonal symmetry, corresponding to a dipole-allowed $\langle OOOE \rangle$ interaction.



General biaxial case

FIG. 6. The general case for the second rank (left) and fourth rank (right) dipole allowed response for an isolated oscillator in biaxial crystals, with k orthogonal to the e_3-e_2 plane. The components in two orthogonal dielectric axes (labelled here A_1 and A_2) are plotted for values of Ψ in the geometry shown in Fig. 3 with a direction k .



Response function formalism for coupled oscillators

$\langle (\hat{\mu}_{0\nu} \cdot \hat{E}_1) (\hat{\mu}_{0\kappa} \cdot \hat{E}_2) (\hat{\mu}_{0\nu} \cdot \hat{E}_3) (\hat{\mu}_{0\kappa} \cdot \hat{E}_4) \rangle \quad \langle (\hat{\mu}_{0\nu} \cdot \hat{E}_1) (\hat{\mu}_{0\nu} \cdot \hat{E}_2) (\hat{\mu}_{0\kappa} \cdot \hat{E}_3) (\hat{\mu}_{0\kappa} \cdot \hat{E}_4) \rangle \quad \langle (\hat{\mu}_{0\nu} \cdot \hat{E}_1) (\hat{\mu}_{0\kappa} \cdot \hat{E}_2) (\hat{\mu}_{\kappa\lambda} \cdot \hat{E}_3) (\hat{\mu}_{\lambda\nu} \cdot \hat{E}_4) \rangle$

 $\langle (\hat{\mu}_{0\nu} \cdot \hat{E}_1) (\hat{\mu}_{0\kappa} \cdot \hat{E}_2) (\hat{\mu}_{0\kappa} \cdot \hat{E}_3) (\hat{\mu}_{0\nu} \cdot \hat{E}_4) \rangle \quad \langle (\hat{\mu}_{0\nu} \cdot \hat{E}_1) (\hat{\mu}_{0\nu} \cdot \hat{E}_2) (\hat{\mu}_{0\kappa} \cdot \hat{E}_3) (\hat{\mu}_{0\kappa} \cdot \hat{E}_4) \rangle \quad \langle (\hat{\mu}_{0\nu} \cdot \hat{E}_1) (\hat{\mu}_{0\kappa} \cdot \hat{E}_2) (\hat{\mu}_{\nu\lambda} \cdot \hat{E}_3) (\hat{\mu}_{\lambda\kappa} \cdot \hat{E}_4) \rangle$

$R_1 \quad R_2 \quad R_3$
 $\begin{pmatrix} 0 & 0 \\ \kappa & 0 \\ \kappa & \nu \\ 0 & \nu \end{pmatrix} \quad \begin{pmatrix} 0 & 0 \\ \kappa & 0 \\ 0 & 0 \\ 0 & \nu \end{pmatrix} \quad \begin{pmatrix} \nu & \nu \\ \lambda & \nu \\ \kappa & \nu \\ 0 & \nu \end{pmatrix}$
 $+ \hat{k}_2 \nearrow \swarrow + \hat{k}_3 \quad + \hat{k}_3 \nearrow \swarrow + \hat{k}_2 \quad + \hat{k}_3 \nearrow \swarrow + \hat{k}_2$
 $- \hat{k}_1 \swarrow \nearrow - \hat{k}_1 \quad - \hat{k}_1 \swarrow \nearrow - \hat{k}_1 \quad - \hat{k}_1 \swarrow \nearrow - \hat{k}_1$

$R_4 \quad R_5 \quad R_6$
 $\begin{pmatrix} 0 & 0 \\ \nu & 0 \\ \nu & \kappa \\ \nu & 0 \end{pmatrix} \quad \begin{pmatrix} 0 & 0 \\ \kappa & 0 \\ 0 & 0 \\ \nu & 0 \end{pmatrix} \quad \begin{pmatrix} \kappa & \kappa \\ \lambda & \kappa \\ \nu & \kappa \\ \nu & 0 \end{pmatrix}$
 $+ \hat{k}_1 \nearrow \swarrow + \hat{k}_3 \quad - \hat{k}_2 \swarrow \nearrow + \hat{k}_3 \quad + \hat{k}_1 \nearrow \swarrow + \hat{k}_3$
 $- \hat{k}_2 \swarrow \nearrow - \hat{k}_2 \quad + \hat{k}_1 \swarrow \nearrow - \hat{k}_2 \quad - \hat{k}_2 \swarrow \nearrow - \hat{k}_2$

UK XFEL Life Sciences Webinar STFC – 28 July 2020 – van Thor

Uniaxial Class						
n	EEEE	OOOO	OEOE EOEO	OOEE EEOO	OEOO EOOE	OOOE EOOO
3	VVVV VKVK VKVK VVKK	VVVV VKVK VKVK VVKK	VVVV VKVK	VVVV VVKK	VVVV VKVK	VVVV
4,6	VVVV VKVK VKVK VVKK	VVVV VKVK VKVK VVKK	VVVV VKVK	VVVV VVKK	VVVV VKVK	

